LC-DET-2014-009
http://www-flc.desy.de/lcnotes

Detailed Simulation of Large Prototype TPC Testbeam Data

Astrid Münnich
DESY, Hamburg

September 29, 2014

Abstract

A simulation describing in detail the charge transfer processes in a GEM stack was used to model data taken with the Large Prototype at the DESY testbeam facility. Comparisons based on signal width and single point resolution will be presented. The simulation is then used to study the single point resolution over long drift distances up to 2.5 m as needed for a TPC at the International Linear Collider.

Contents

1 Simulation Framework

A simulation framework has been developed to describe in detail the charge transfer processes in a GEM stack [1]. Good agreement between simulation and prototype data was demonstrated for the gas mixtures P5 (Ar(95%),CH_4(5%)) and TDR (Ar(93%),CH_4(5%),CO_2(2%)) [1]. The framework is implemented in MarlinTPC [2] and consists of several modules available as Marlin processors [3]:

1. Primary Ionization:
   According to parametrizations obtained with HEED [4] electrons are placed along the charged particle track.

2. Drift:
   The drifting of electrons is done in a simple way based on gas properties obtained from a parametrization of MAGBOLTZ [5] simulations.

3. Amplification with GEMs:
   The charge transfer in the GEM stack is modeled following the results from detailed current measurements on all electrodes [6].

4. Charge distribution on pad plane:
   The charge cloud created in the amplification process is distributed on the pad plane by integrating a two dimensional Gaussian with a width given by the diffusion in the GEM stack.

5. Electronics:
   The last step is the simulation of the shaper and ADC to generate a raw data signal that has the same format as real data.

This framework is now used to model data taken with the Large Prototype at the DESY testbeam facility with the T2K gas mixture (Ar(95%),CF_4(3%),iC_4H_{10}(2%)).

1.1 Testbeam Setup and Data Sets

The Large Prototype (LP) has been built within the LCTPC collaboration [7, 8] to compare different readout modules under identical conditions and to address integration issues. The field cage has a length of 61 cm and a diameter of 72 cm. It can reach a cathode voltage of up to 24 kV which corresponds to drift fields up to 350 V/cm which is sufficient for common gases. Composite materials were used to achieve a low material budget of 1.24 % of a radiation length X_0 per wall [9].

The endplate can hold up to seven modules each with a size of about $22 \times 17\,\mathrm{cm}^2$. The design of the endplate and the module placement resembles a cut out of a large scale endplate. A picture of the endplate is shown in Fig. 1 on the left showing three of the slots equipped with GEM modules and the remaining four with termination shield modules.

The DESY test beam facility [10] provides an $e^{\pm}$ beam with particle momenta up to 6 GeV. A 1 T magnet with a bore large enough to fit the LP is available. The magnet is mounted on a movable stage, enabling a movement of the setup around three axes. A test beam campaign has been carried out with three modules [11].

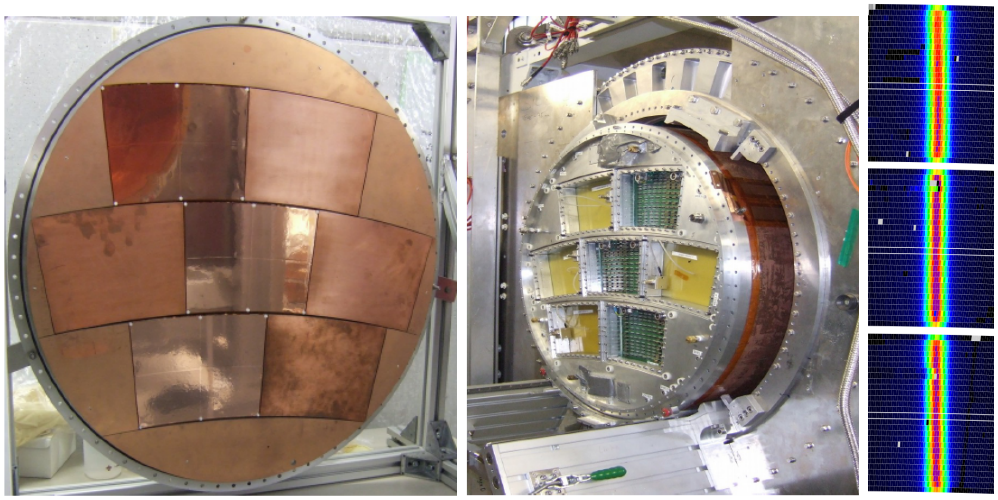

Figure 1: Three GEM modules were installed in the endplate visible in the left picture as the shiny surfaces. The middle picture shows the LP inserted into the magnet before the electronics is attached. On the right an integrated beam profile is shown crossing the three modules.

Although the full module area is equipped with readout pads only one half of each module is equipped with electronics due to a limited amount of available channels and space constraints. Pads that are not connected to a readout channel are grounded. In total 7200 channels were read out using the ALTRO electronics [12] with a shaping time of 120 ns. A lever arm of about 50 cm along the beam was achieved with this configuration as shown in Fig. 1.

The data sets considered here have been taken using the T2K gas mixture. A z scan with over ten different drift distances has been taken at 0 T and 1 T magnetic field. The beam momentum of the electrons was set to 5 GeV.

1.2 Simulation Setup

Electron tracks of 5 GeV were created at different z positions in the chamber with a position smearing corresponding to the beam profile. The gas mixture and GEM settings were the same as in the measurements.

2 Comparison with LP Data

As there is no calibration of the electronics available, the dynamic range of the ADC in the simulation was adjusted to match the charge spectra observed in data. The comparison of the hit charge in dependence on the drift distance is shown in Fig. 2 for simulation and measured data at 0 T and 1 T.

2.1 Pad Response Function

The width of the charge cloud arriving on the pad plane is dominated by the diffusion between the GEMs and in the induction gap. However, there are effects visible in the

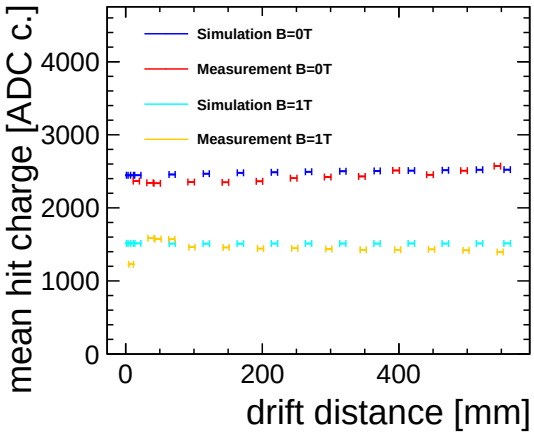

Figure 2: Hit charge in dependence on the drift distance for simulation and measurement, each at 0 T and 1 T.

data caused by induction on neighboring pads. The pad response function describes this width and shows non Gaussian tails due to this induction. In order to determine the amount of induction, the simulation was carried out with 0, 10 and 20% of charge induction to the neighbouding pads. The result is shown in Fig. 3.

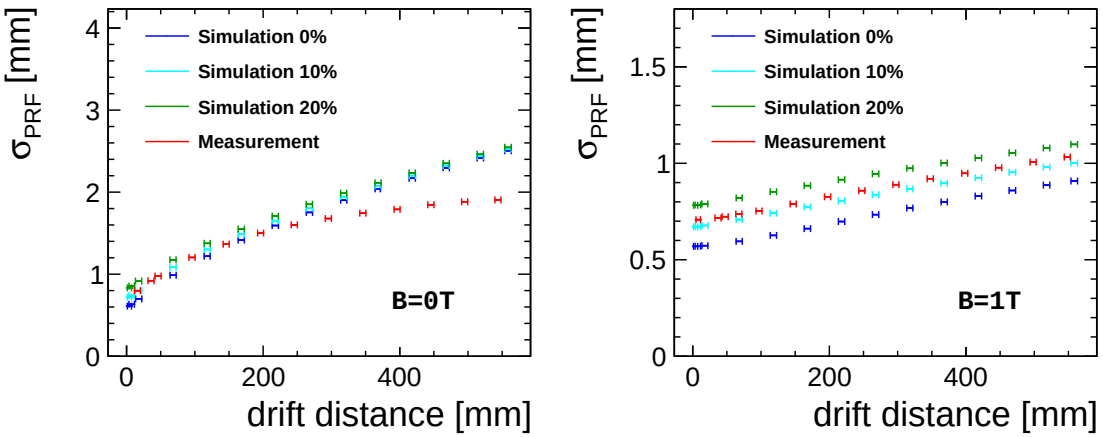

Figure 3: Dependence of the PRF width on the drift distance for different amounts of induction in the simulation without magnetic field (left) and for 1 T magnetic field (right).

Without magnetic field the diffusion is dominating the PRF and no significant change is observed. In comparison a drop in PRF width compared to the simulation is observed in the data. The origin of this unexpected decrease is under investigation. It is likely the same effect that causes the resolution to fall below the expected root behaviour as will be discussed in section 2.2.1. In case of 1 T however the contribution of induction to the PRF width becomes visible. For the following results an induction of 10% was chosen in the simulation, since it fits the data best. Another observation from the right plot in Fig. 3 is that the PRF width at zero drift distance is higher than the value expected from the diffusion only, even for 0% induction. This can be explained by the finite pad size. The left plot in Fig. 4 shows

a comparison of the shape of the PRF response in data and simulation with a good agreement. The right plot in Fig. 4 shows the dependence of $\sigma_{\mathrm{PRF}}(z = 0)$ on the pad width. The expected diffusion value, in this case an input width of 0.36 mm was used, can only be achieved for very thin pads. For a pad width of 1.26 mm the value of $\sigma_{\mathrm{PRF}}(z = 0)$ has risen significantly. The diffusion limit inside the GEM stack can be derived from $\sigma_0^2 = \sigma_{\mathrm{PRF}}(z = 0)^2 + w^2/12$ where w is the pad width. This functionality is fitted in the right plot of Fig. 4 with very good agreement.

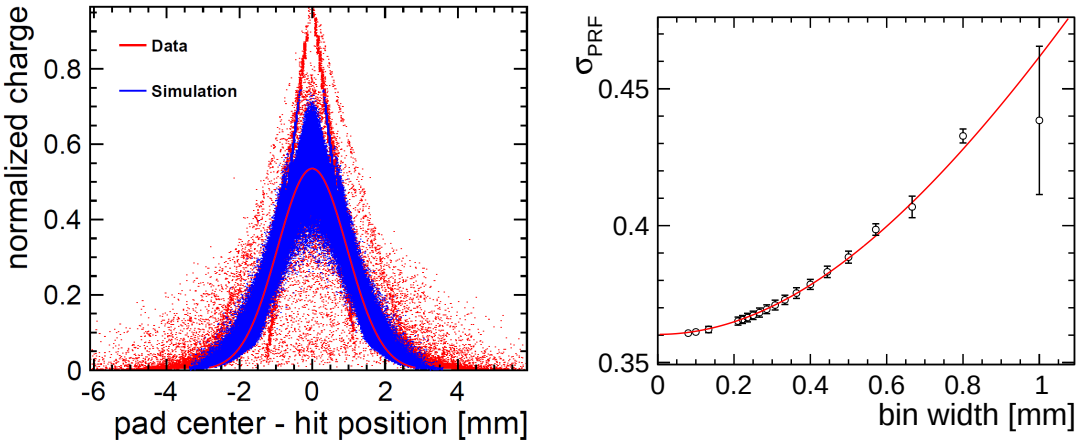

Figure 4: Comparison of the PRF shape (left) and result from a toy MC to illustrate the effect of a finite pad width on $\sigma_{\mathrm{PRF}}(z = 0)$.

2.2 Single Point Resolution

The single point resolution describes the distance of a hit to its track. As we lack an external reference, one way to limit the bias of this definition is to evaluate the distance of the point to the track once with the point included in the fit (σ_{res}) and once without (σ_{dist}). The resolution is then given by $\sigma = \sqrt{\sigma_{\mathrm{res}}\sigma_{\mathrm{dist}}}$. The resolution is evaluated separately in the two projections $r\phi$ and z.

2.2.1 $r\phi$ Plane

The distance of the points to the track follows a Gaussian distribution whose width is increasing with larger drift distances due to the transverse diffusion. An example is shown in Fig. 5.

The resolution curve shows the dependence on the drift distance as shown in Fig. 6. Without magnetic field the diffusion is larger therefore the resolution is worse. The drift dependence can be described by $\sigma = \sqrt{\sigma_0^2 + D_t^2/N_{\mathrm{eff}}}$ where D_t is the transverse diffusion and N_{eff} the number of primary electrons per pad row. σ_0 describes the limit in resolution that can be achieved at zero drift length.

Without magnetic field the discrepancy between simulation and measurement is larger. The simulation follows the expected root law perfectly whereas the data flattens out after 200 mm of drift. We do not have an explanation for this effect yet. The resolution curves at 1 T show much better agreement. But also here the

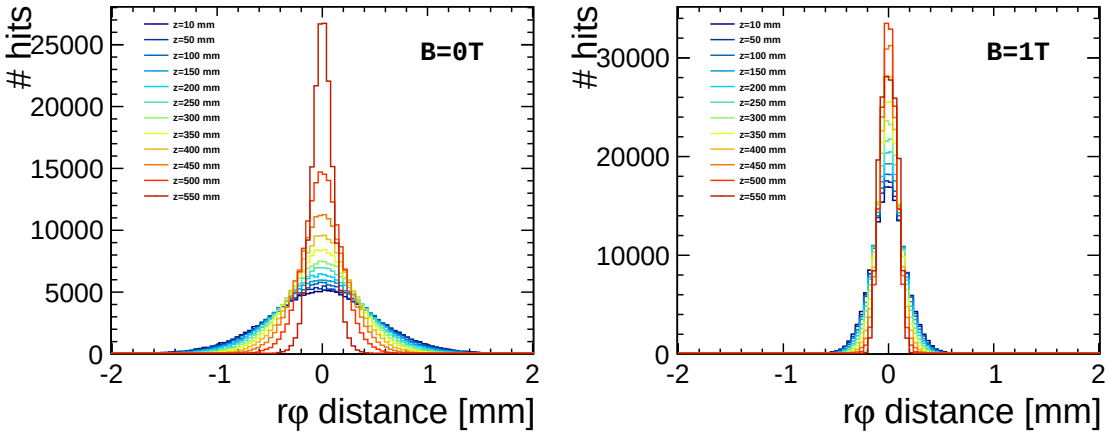

Figure 5: Distribution of the distance of each point in the $r\phi$ plane to the track at different drift distances without magnetic field (left) and at 1 T (right).

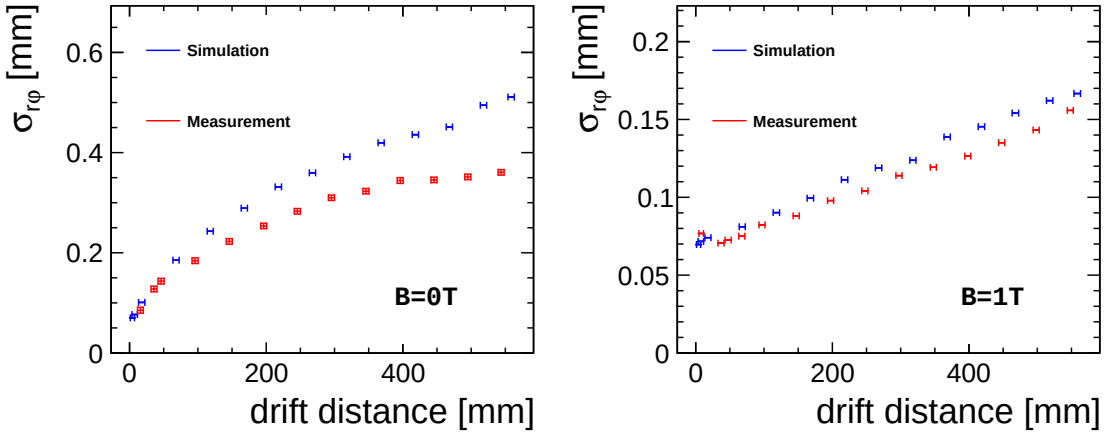

Figure 6: Single point resolution in the $r\phi$ plane for simulation and data without magnetic field (left) and for 1 T (right).

measurement shows a tendency to flatten at longer drift distances compared to the simulation.

Fig. 7 shows a comparison of the resolution of the best row for different data sets including results from testbeam campaigns with Micromegas modules. The simulation agrees rather well with the data set of the Micromegas from 2013. But the main point to observe is that we do see a spread in the data of the measurements between different testbeam campaigns which might be due to environmental changes and gas quality. These factors are not included in the simulation which assumes perfect conditions.

2.2.2 z Direction

The resolution in the z direction is dominated by the shaping of the electronics. In our case for the ALTRO electronics the shaper creates a so called Gamma4 function:

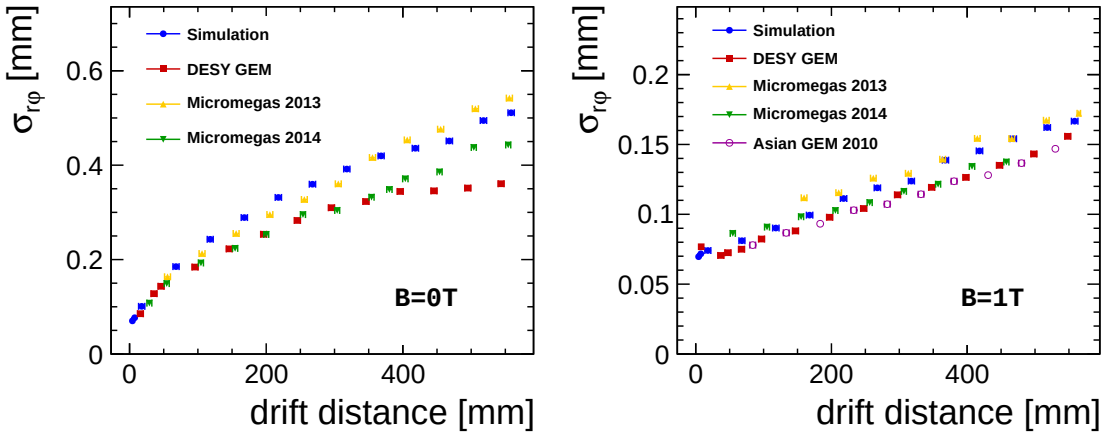

Figure 7: Single point resolution in the $r\phi$ plane for simulation and different data sets without magnetic field (left) and for 1 T (right).

$$f(A, t_0, \tau, k, t) = Ae^k \left(\frac{t - t_0}{\tau}\right)^k \exp -k\frac{t - t_0}{\tau}\theta(t - t_0) \tag{1}$$

where A is the amplitude, t_0 the starting time and τ the peaking time. k is fixed by the electronics to 4, hence the name Gamma4 function. In the simulation this function is used to distribute the charge cloud into the time bins of the ADC. Each electron cloud creates one Gamma4 function, overlapping bins are added. The overall pulse shape can be reproduced as can be seen in Fig. 8. As expected, it does not depend on the magnetic field. In the data however, many pulses do not have a perfect shape. The electronics seems to be sensitive to changes in charge and shape which can not be modeled in the simulation due to the lack of information about the electronics response.

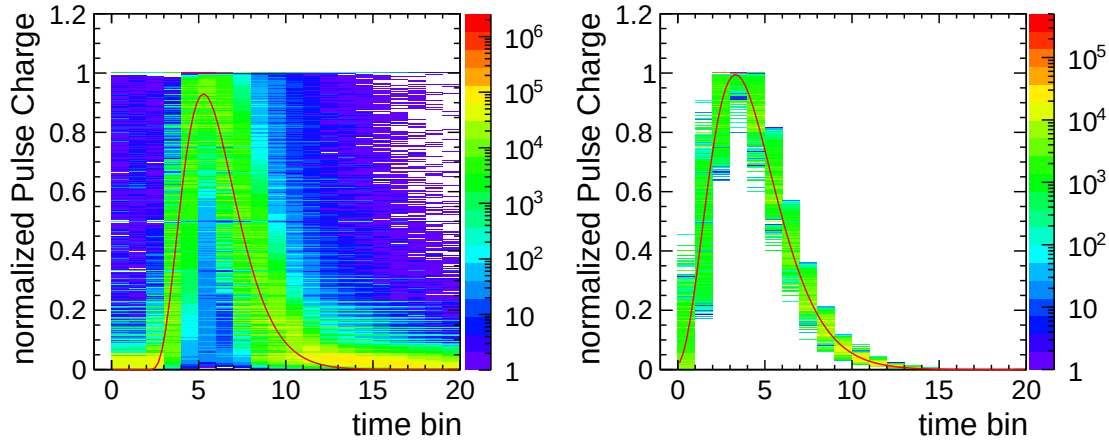

Figure 8: Example of a normalized pulse shape for data (left) and simulation (right).

When comparing the resolution in the z direction (Fig. 9 and Fig. 10) it is obvious that there is a large discrepancy between the simulation and the measurement.

The simulation shows a large variation in the width of the resolution distribution as function of the drift distance (Fig. 9 left) whereas in the data almost no drift dependence is observed (Fig. 9 right).

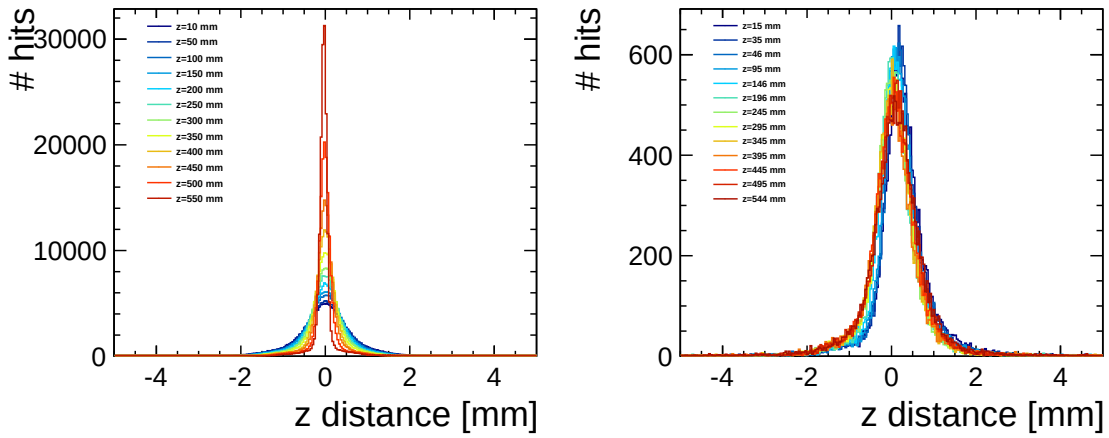

Figure 9: Distribution of the distance of each point in the z plane to the track at different drift distances without magnetic field for the simulation (left) and the measurement (right).

This is also reflected in Fig. 10 where the z resolution is shown versus the drift distance. The simulation follows the expected root law due to the longitudinal diffusion whereas the measured points stay rather flat over the full drift distance.

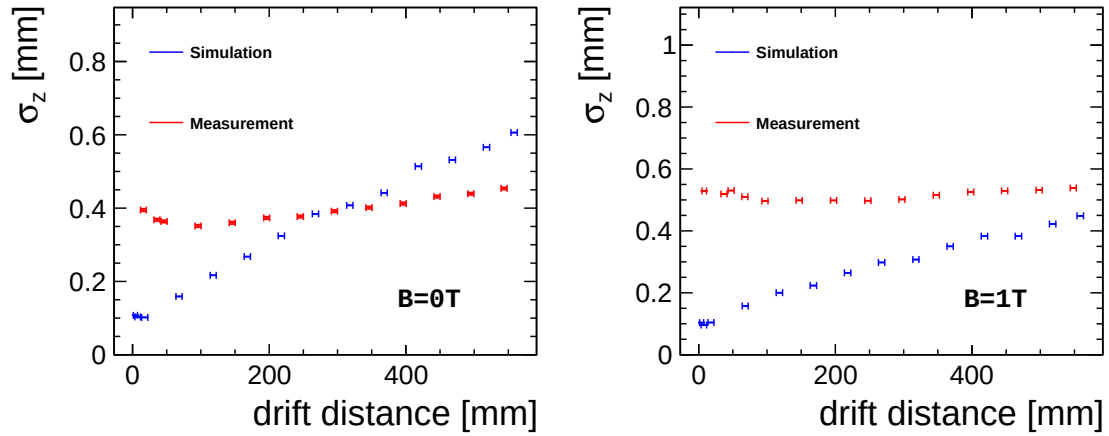

Figure 10: Single point resolution in the z direction for simulation and data without magnetic field (left) and for 1 T (right).

When comparing the z resolution with data sets from different testbeam campaigns and LP modules, Fig. 11, one can observe that the Micromegas data shows the same slope behavior even though a different electronics is used. For a magnetic field of 1 T, we have a data set with the Asian GEM module that also uses the ALTRO electronics. Here, the z resolution is better than for the DESY GEM module but also rather flat which can not be reproduced in the simulation.

At first glance it is however strange that there is a difference visible in the simulation between 0 T and 1 T as the magnetic field has no influence on the longitudinal

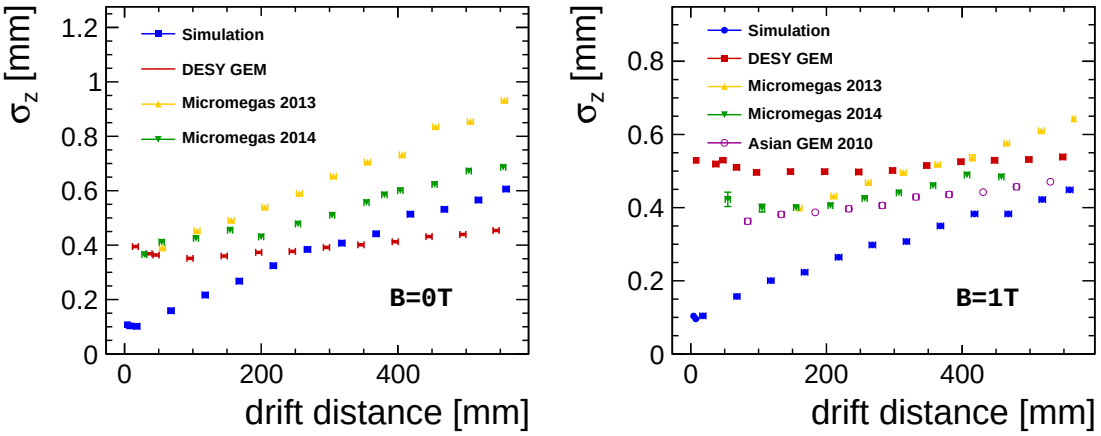

Figure 11: Single point resolution in the z direction for simulation and different data sets without magnetic field (left) and for 1 T (right).

diffusion. It can however be seen that also the transverse diffusion has an impact on the z resolution. This might be correlated to a charge effect as the charge is narrower with magnetic field in the transverse plane and therefore more charge is collected on a channel. This effect is shown in the left plot of Fig. 12 depicting the normalized maximum charge of the pulses illustrating that the number of larger pulses is much increased with magnetic field. As the time of the hit is evaluated from the largest pulse in that hit the time estimation therefore benefits from larger pulses and thus improves the time resolution. The right plot in Fig. 12 shows the slight improvement in the z resolution when reducing the transverse diffusion by 20%. The difference in transverse diffusion when going from 0 T to 1 T is more than a factor 3. The only way to reproduce the flat behaviour of the data is to turn off the longitudinal diffusion in the simulation. This gives a flat response in the simulation but at a lower level which represents then the resolution limit due to the electronics capabilities. We suspect that there is some part in the electronics that dominates over the fact that the charge is spread out in time, maybe in the way the charge up is done which is not fully understood yet and therefore can not be modeled ralistically in the simulation.

To verify the dependence of the z resolution on the pulse charge the resolution is evaluated separately for 3 different charge regions:

1. Low charge: charge of maximum pulse between 0 and 100 ADC counts
2. Medium charge: charge of maximum pulse between 100 and 200 ADC counts
3. High charge: charge of maximum pulse above 200 ADC counts

The maximum charge value that can be reached with this electronics is around 900 ADC counts whereas the mean pulse charge is about 100 ADC counts. The result is shown in Fig. 13. The larger the maximum charge of the pulse in a hit the better the resolution in both measurement directions. The same result is obtained with magnetic field.

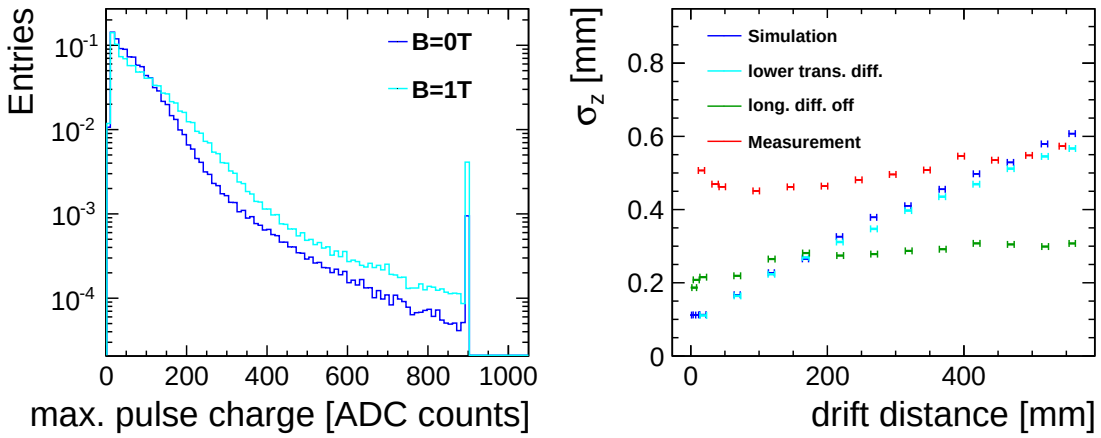

Figure 12: Distribution of maximum charge in a pulse with and without magnetic field (left). z resolution for simulation with nominal, low and without longitudinal diffusion without magnetic field in comparison with the measurement.

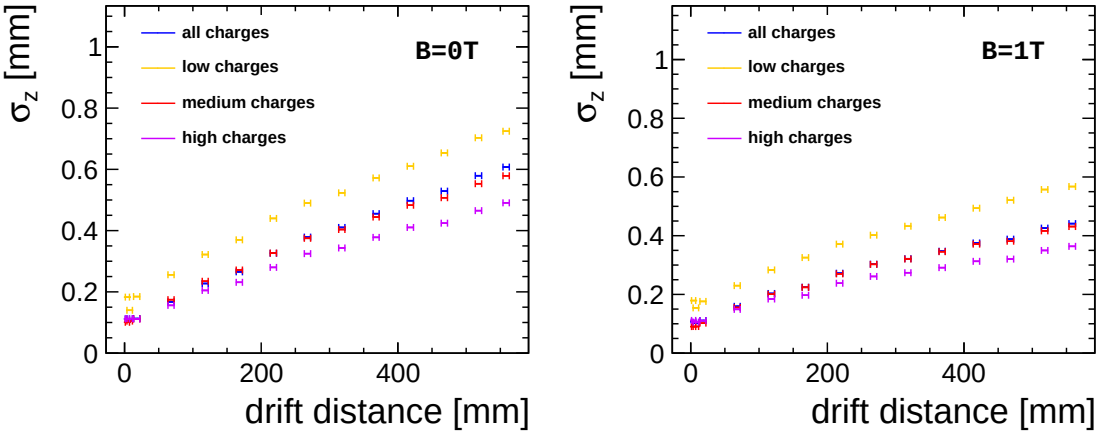

Figure 13: Dependence of the resolution in z on the maximum pulse charge in a hit without magnetic field (left) and at 1 T (right).

3 Extrapolation to Large Drift Distances

The single point resolution goal for a TPC at the ILC is $\sim 100\,\mu$m over the full drift length to provide the required momentum resolution. Currently a magnetic field of 3.5 T is foreseen. The simulation of the 3 modules in the Large Prototype was extended to large drift distances of up to 2.5 m. Different pad sizes and layouts were simulated. The result is shown in Fig. 14 which shows that a pad size currently implemented on the LP modules is almost sufficient especially if the pad response correction is applied. With a pad width of 1 mm however the goal can be reached even without such a correction.

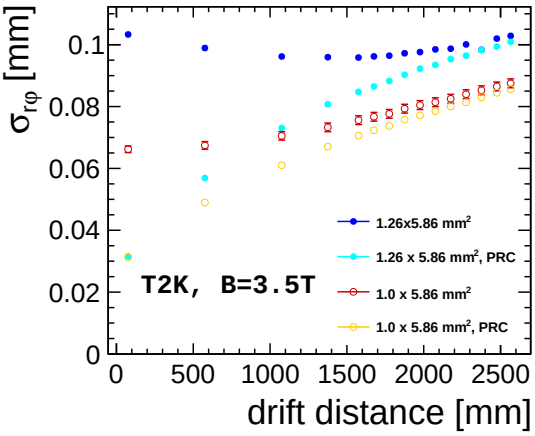

Figure 14: Single point resolution in $r\phi$ plane at 3.5 T for different pad geometries over the full length of an ILD sized TPC.

4 Summary and Outlook

The detailed GEM simulation is able to reproduce data taken with TDR and P5 with and without magnetic field. The agreement between simulation and data for T2K gas is less good. Effects seen in the data need to be better understood, like e.g. the drop in the single point resolution in the $r\phi$-plane. In order to further improve the simulation, a parametrization of the charge transfer coefficients for T2K at 4T would be helpful. Due to the CF_4 contribution, T2K gas is difficult to simulate. Those difficulties are not only observed in the detailed GEM simulation but also in programs like MAGBOLTZ and Garfield [14] which provide the necessary input parameters for the simulation. The electrostatic parametrization to describe the charge transfer coefficients in a GEM stack also does not fit well anymore for the T2K gas mixture.

Furthermore, additional information about the electronic response would be needed to model the ALTRO electronics correctly in the simulation. If the charge cloud is small compared to the pad width, the details of the electronics behavior do not only influence the measurement in the z direction, but also the resolution in the $r\phi$ plane as small pulses on side pads might be lost.

References

[1] A. Münnich, *Simulation studies for a high resolution time projection chamber at the international linear collider*, Aachen, Techn. Hochsch., Diss., 2007

[2] Christoph Rosemann, Executive Summary: *Recent Software Developments for Time Projection Chambers*, LC-DET-2012-071, 2012,
MarlinTPC homepage. `https://znwiki3.ifh.de/MarlinTPC/`

[3] MARLIN homepage. `http://ilcsoft.desy.de/marlin`

[4] I. Smirnov, *HEED: Interactions of particles with gases*, W5060, http://consult.cern.ch/writeup/heed/

[5] S.Biagi, *MAGBOLTZ: Transport of electrons in gas mixtures*, http://consult.cern.ch/writeup/magboltz/

[6] M. Killenberg et al., Nucl. Instr. Meth. A498 (2003) 369

[7] Homepage of the LCTPC collaboration, http://www.lctpc.org

[8] R. Diener on behalf of the LCTPC collaboration, *Development of a TPC for an ILC Detector*, *Physics Procedia* **37** (2012) 456-463

[9] T. Behnke, K. Dehmelt, R. Diener, L. Steder, T. Matsuda, V. Prahl and P. Schade, *A lightweight field cage for a large TPC prototype for the ILC*, 2010 JINST 5 P10011

[10] DESY test beam information. http://testbeam.desy.de/

[11] T. Behnke et al 2013 JINST 8 C10010, doi:10.1088/1748-0221/8/10/C10010

[12] L.Joensson, U.Mjoernmark, *Front-end electronics and data acquisition for the LCTPC*, Eudet-Memo-2007-53

[13] Ralf Diener, *Study of Reconstruction Methods for a Time Projection Chamber with GEM Gas Amplification System*, DESY-THESIS-2006-040

[14] Garfield++ project web page , http://garfieldpp.web.cern.ch/garfieldpp/